Seismocardiography-Based Detection of Cardiac Quiescence for Cardiac Computed Tomography Angiography

Carson A. Wick[1], *Member*, *IEEE*, James H. McClellan[1], *Fellow*, *IEEE*,
Omer T. Inan[1], *Member*, *IEEE*, and Srini Tridandapani[2], *Member*, *IEEE*

***Abstract*— As a measure of chest wall acceleration caused by cardiac motion, the seismocardiogram (SCG) has the potential to supplement the electrocardiogram (ECG) to more accurately trigger cardiac computed tomography angiography (CTA) data acquisition during periods of cardiac quiescence. The SCG was used to identify the systolic and diastolic quiescent periods of the cardiac cycle on a beat-by-beat basis and from composite velocity signals for nine healthy subjects. The cardiac velocity transmitted to the chest wall was calculated using a Kalman filter. The average systolic and diastolic quiescent periods were centered at 30% and 76%, respectively. Inter- and intra-subject variability of the quiescent phases with respect to the ECG was observed, suggesting that the ECG may be a suboptimal modality for predicting cardiac quiescence.**

I. INTRODUCTION

Cardiac computed tomography angiography (CTA) is a promising technique for diagnosing coronary artery disease, which can be attributed to one in every six deaths in the United States of America [1]. CTA is considerably less invasive and more cost effective than the current gold standard for diagnosing coronary artery disease, the catheterized coronary angiogram. However, CTA requires that imaging data be acquired during periods of minimal cardiac motion within the cycle to obtain motion-free images. Therefore, it is imperative to accurately trigger computed tomography (CT) data acquisition during periods of cardiac quiescence.

The current method for predicting cardiac quiescence, the electrocardiogram (ECG), is an indirect representation of the mechanical state of the heart. As a direct representation of chest wall motion due to cardiac activity, seismocardiography (SCG) can be used as a marker of cardiac quiescence and may prove more reliable than the ECG for the prediction of cardiac quiescent periods [2]–[5].

For this work, cardiac quiescence is determined from periods of minimal velocity magnitude derived from the SCG acceleration signal. Acceleration cannot be used directly because periods of minimal acceleration could potentially correspond to periods of constant velocity. Although SCG is a one-dimensional representation of cardiac motion, it is CT-compatible in that SCG measurement devices, linear accelerometers, can be introduced into the CT scanner without causing significant streak artifacts in the CT images. Furthermore, SCG can be used for the real-time prediction of cardiac quiescence. Therefore, SCG has strong potential to supplement ECG as a signal for cardiac gating of imaging data acquisition.

The remainder of this paper is organized as follows. Section II presents the methods used for quiescent period identification. Periods are detected on a beat-by-beat basis and from composite velocity signals. The results of the detection methods for nine patients are provided in Section III. Lastly, a short discussion of the impact and applicability of the proposed methods is given in Section IV.

II. METHODS

Cardiac quiescence is detected from the SCG on a beat-by-beat basis and from composite velocity signals. A Kalman filter is used to obtain a robust estimate of the cardiac motion transmitted to the chest wall velocity in real-time from the SCG. The magnitude of this velocity is then estimated using a sliding window root mean square (RMS) technique. From the velocity magnitude, quiescence is detected on a beat-by-beat basis. Lastly, to obtain a more robust indication of the velocity magnitude on average as a function of heart rate for each patient, the observed cardiac cycles are sorted by their instantaneous heart rates and averaged to form composite signals. Quiescent period phases and durations are then calculated from these composite signals.

A. Beat-by-Beat Detection of Cardiac Quiescence from SCG

Cardiac quiescence is detected from the SCG as periods of minimal velocity by using a Kalman filter to calculate the cardiac velocity transmitted to the chest wall from the acceleration provided by the SCG. The Kalman filter framework provides a robust method for estimating the underlying true acceleration and velocity from the potentially noisy SCG [6], [7]. Quiescence will be defined as periods of minimal velocity.

Velocity is estimated in real-time from the acceleration signal provided by the SCG, $a(i)$, using a Kalman filter. The model state is defined as

$$\mathbf{x}(i) = \begin{bmatrix} x(i) & v(i) & a(i) & j(i) \end{bmatrix}^T, \tag{1}$$

where $x(i)$ is the position, $v(i)$ is the velocity, $a(i)$ is the acceleration, and $j(i)$ is the jerk of the SCG accelerometer

This work was supported in part by Award Number K23EB013221 from the National Institute of Biomedical Imaging and Bioengineering. The work of J. H. McClellan was supported by the John and Marilu McCarty Chair.

[1]C. A. Wick, J. H. McClellan, and O. T. Inan are with the School of Electrical and Computer Engineering, Georgia Institute of Technology, Atlanta, GA 30332, USA.

[2]S. Tridandapani [stridan@emory.edu] is with the Department of Radiology and Imaging Sciences, Emory University, Winship Cancer Institute, Atlanta, GA 30322, USA.

978-1-4244-7929-0/14/$26.00 ©2014 IEEE

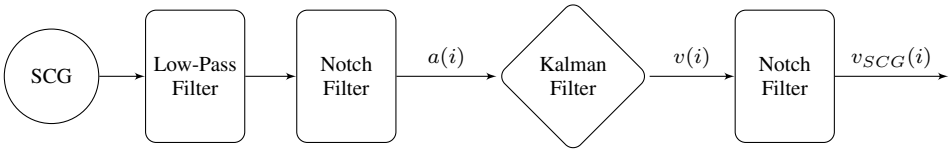

Fig. 1. Signal processing flow to determine chest wall velocity from the SCG.

sensor. The update equations can then be defined as

$$x(i) = x(i-1) + v(i-1)\Delta t + a(i-1)\frac{\Delta t^2}{2} + j(i-1)\frac{\Delta t^3}{6}, \quad (2a)$$

$$v(i) = v(i-1) + a(i-1)\Delta t + j(i-1)\frac{\Delta t^2}{2}, \quad (2b)$$

$$a(i) = a(i-1) + j(i-1)\Delta t, \quad (2c)$$

$$j(i) = j(i-1), \quad (2d)$$

where Δt is the sampling period. By introducing jerk into the model, the accuracy of $a(i)$ will increase because the assumption of constant acceleration between samples is no longer necessary. Although (2d) indicates that jerk is constant, this is not the case. The resulting model error in the jerk term can be accommodated by setting the process error associated with the jerk term equal to the expected variance of the jerk.

The Kalman update equation for this model is defined as

$$\mathbf{x}(i) = \mathbf{A}\mathbf{x}(i-1) + \mathbf{w}, \quad (3)$$

where $\mathbf{A}$ is the state transition matrix and $\mathbf{w}$ is the process error. Next, the observation equation is defined as

$$\mathbf{z}(i) = \mathbf{H}\mathbf{x}(i) + \mathbf{v}, \quad (4)$$

where $\mathbf{z}(i)$ is the observation, $\mathbf{H}$ is the measurement matrix, and $\mathbf{v}$ is the measurement noise at time index i.

The update equations, defined by (2), result in a state-transition matrix of

$$\mathbf{A} = \begin{bmatrix} 1 & \Delta t & \frac{\Delta t^2}{2} & \frac{\Delta t^3}{6} \\ 0 & 1 & \Delta t & \frac{\Delta t^2}{2} \\ 0 & 0 & 1 & \Delta t \\ 0 & 0 & 0 & 1 \end{bmatrix}. \quad (5)$$

The jerk term of the process error, $\mathbf{w}$, will be equal to the variance of dj/dt. This variance is approximated by computing the variance of $a(i+1) - 2a(i) + a(i-1)$.

Because only acceleration is measured by SCG, the measurement matrix will be

$$\mathbf{H} = \begin{bmatrix} 0 & 0 & 1 & 0 \end{bmatrix}, \quad (6)$$

and the measurement error, $\mathbf{v}$, is equal to the variance of the signal noise in $a(i)$.

The velocity of the chest wall, $v_{SCG}(i)$, is calculated from the SCG signal using a combination of low-pass, notch, and Kalman filters. The SCG signal is first low-pass filtered with a cutoff of 20 Hz to remove higher frequency content associated with the sounds of the cardiac valves [8]. The resulting signal is then passed through a notch filter centered at 0 Hz with a cutoff of approximately 2 Hz to remove any DC offset and respiratory motion. The resulting signal, $a(i)$, is then passed through a Kalman filter to obtain a robust estimation of the chest wall velocity, $v(i)$. The velocity is then passed through a notch filter equivalent to the first to remove any lingering DC bias. This process is summarized in Fig. 1.

The approximate magnitude of the chest wall velocity, $\hat{v}_{SCG}(i)$, is calculated as the windowed RMS of $v_{SCG}(i)$. An 83 ms rectangular window is used for two reasons. First, the resulting signal will be a smoothed version of the velocity magnitude of the chest wall, making identification of quiescent periods easier. Second, an 83 ms window corresponds to the typical data acquisition time of a single slice on a dual-source CT scanner, such as the Siemens SOMATOM Definition Flash (Siemens Healthcare, Erlangen, Germany). Each value of $\hat{v}_{SCG}(i)$ corresponds to the RMS of the chest wall velocity for a length of time corresponding to the CT slice data acquisition time centered at i. The windowed RMS is calculated as

$$\hat{v}_{SCG}(i) = \sqrt{\frac{1}{N}\sum_{n=-N/2}^{N/2} v_{SCG}^2(i+n)}, \quad (7)$$

where N is is the number of samples corresponding to 83 ms. An example of $v_{SCG}(i)$ and $\hat{v}_{SCG}(i)$ along with the synchronized ECG are shown in Fig. 2. Quiescent periods are determined as time intervals where $\hat{v}_{SCG}(i)$ is less than the mean of $\hat{v}_{SCG}$ for each cardiac cycle as defined by the synchronously acquired ECG.

B. Quiescence from Composite Velocity Signals

To identify the overall nature of cardiac quiescence from SCG for a range of observed heart rates, composite velocity magnitude signals are generated for each subject. These composite signals are created by segmenting the velocity magnitude signal, $\hat{v}_{SCG}(i)$, by the R-R interval of the synchronously recorded ECG signal. After segmentation, the instantaneous heart rate for each cycle is derived from the known cycle length in seconds. Cycles of the velocity magnitude signal can then be sorted into groups by the instantaneous heart rate of each cycle. After sorting, the segmented cycles are time-scaled to equal length, allowing the groups to be averaged and compared. This process is summarized as

$$\overline{v}_m(i) = \frac{1}{N_m}\sum_{\hat{v}_n \in H_m} \hat{v}_n(i), \quad (8)$$

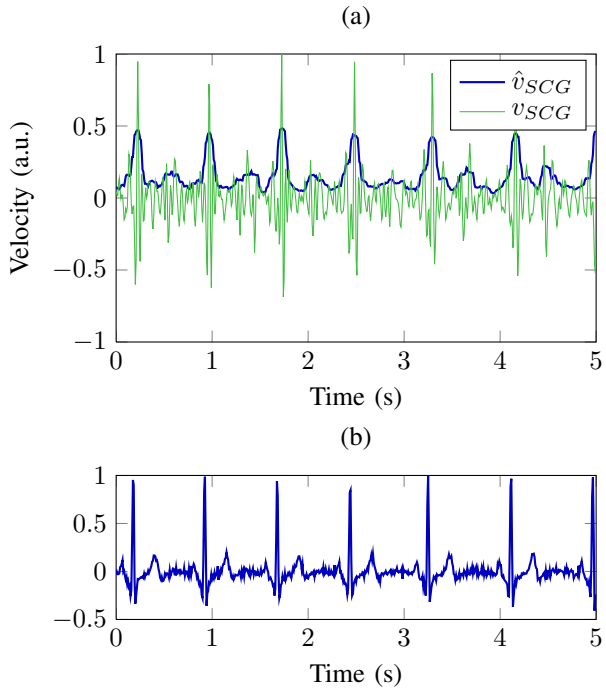

Fig. 2. Plot of chest wall velocity, v_{SCG}, and velocity magnitude, $\hat{v}_{SCG}$, from the SCG (a) along with the synchronized ECG (b).

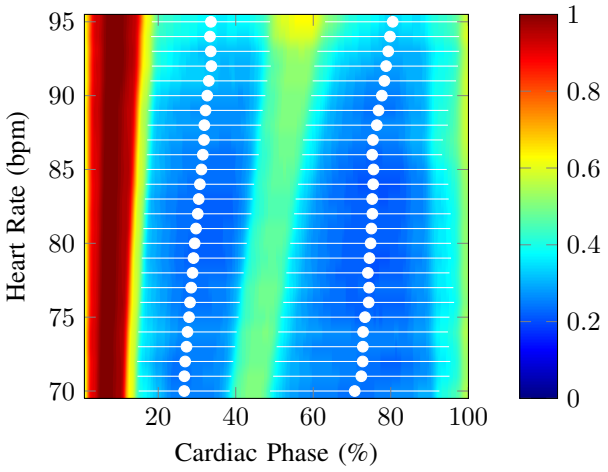

Fig. 3. Image of composite velocity magnitudes, $\overline{v}_m(i)$, across a range of heart rates for Subject 7. The longest systolic (left) and diastolic (right) quiescent periods are indicated in white. The center of each quiescent period is indicated by a white circle and the duration is indicated by the line passing through that circle.

where $\overline{v}_m(i)$ is the composite velocity magnitude signal for heart rate range H_m, N_m is the number of cycles in the range H_m, and $\hat{v}_n(i)$ is the n^{th} time-scaled velocity magnitude cycle in H_m. Quiescent periods can be determined from each $\overline{v}_m(i)$ providing cardiac quiescence information as a function of instantaneous heart rate for each subject. Similar to beat-by-beat detection presented in Section II-A, quiescent periods are detected as time intervals when $\overline{v}_m(i)$ is less that the mean of $\overline{v}_m(i)$.

C. Data Acquisition

Quiescent periods were detected from the SCG for nine healthy human subjects. SCG and ECG data were synchronously acquired for nine healthy human subjects at a rate of 1.2 kHz using a custom SCG acquisition device described in [5]. The SCG sensor was placed at the end of sternum superior to the xiphoid process and acceleration was measured in the dorso-ventral direction. Full informed consent was obtained from each subject in accordance with the Emory University Institutional Review Board. Two of the subjects were examined solely for the SCG. The SCG data of the remaining seven subjects were acquired continuously while the patient received a synchronously acquired echocardiogram.

III. Results

For each subject, the systolic and diastolic quiescent periods were identified on a beat-by-beat basis. Composite velocity magnitude signals were then computed across the range of observed heart rates. Lastly, composite velocity maps and the corresponding quiescent periods were generated for each subject.

The systolic and diastolic quiescent periods were identified for each cardiac cycle using the methods presented in Section II-A. The systolic quiescent period was defined as the longest quiescent period with a center occurring before 60% of the cardiac cycle as defined by the R-R interval of the ECG. The diastolic quiescent period was defined in the same manner but with a center occurring at or later than 60%. A summary of the identified quiescent periods is provided in Table I.

From Table I, the duration of the diastolic periods (in ms) can be seen to decrease with heart rate, while that of the systolic periods is relatively independent of heart rate. These results agree with those demonstrated by [9].

In addition to beat-by-beat detection, quiescent periods were identified for composite velocity magnitude signals using the methods of Section II-B. For each subject, composite velocity magnitude signals, $\overline{v}_m(i)$ from (8), were generated for heart rate range sets with a width of two beats per minute and 50% overlap at one beat per minute increments. All $\overline{v}_m(i)$ were normalized to have a maximum of one. A composite velocity map of all $\overline{v}_m(i)$ for Subject 7 is provided in Fig. 3 with the image intensity corresponding to the velocity magnitude. Quiescent periods were identified for each $\overline{v}_m(i)$ and are indicated on the image in white. Each composite signal represents the average of all velocity magnitude segments with an instantaneous heart rate within ± 1 bpm of the rate indicated. From Figure 3, the duration of the quiescent period during mid-diastole decreases as heart rate increases, whereas the duration of the quiescent period during end-systole increases minimally as heart rate increases.

TABLE I
QUIESCENT PERIOD STATISTICS

Subject	Cycles	Heart Rate	Systolic Periods		Diastolic Periods	
			Center (%)	Duration (ms)	Center (%)	Duration (ms)
1	210	49.6±5.0	22.0± 2.1	161± 8	71.3±2.8	543± 81
2	91	52.0±3.2	24.6± 1.3	132±24	69.5±1.5	639± 50
3	3820	63.9±5.4	30.8±12.8	162±83	76.6±9.2	281±135
4	3801	67.1±6.3	29.5± 6.7	183±54	77.4±6.5	348±114
5	3509	68.4±8.6	30.9± 9.7	187±80	75.9±8.9	322±158
6	3041	74.1±6.5	31.7± 7.5	135±54	75.5±6.3	324±106
7	6445	81.5±6.8	30.8± 6.3	191±54	76.2±6.3	263± 91
8	4481	84.7±3.4	31.1±10.7	129±50	80.8±4.5	236± 56
9	1759	90.1±5.1	32.7± 4.5	173±44	77.9±4.7	227± 62

IV. DISCUSSION

The two methods presented above address the problem of quiescent period detection using two different approaches. The beat-by-beat detection method presented in Section II-A is an approach that can be used to detect quiescence in real-time. The downside to this approach is that it is subject to sensor noise and subject movement. The composite signal method for detecting quiescent periods presented in Section II-B relies on generating typical velocity magnitude signals for the range of heart rates observed for each patient. Because this method relies on averaging many signals together it is more robust at the expense of not being sensitive to beat-by-beat variation in the motion of the chest wall.

Beat-by-beat detection can be used to observe quiescence in real-time with minimal delay. Although this method is sensitive to patient movement, the expected level of patient movement during a CT exam should be similar to that observed for Subject 1 and 2 who were examined solely for SCG acquisition. The results for the remaining subjects demonstrate more noise in terms of standard deviation. It is assumed that this is partly the result of patient motion due to the simultaneous echocardiography exam each of those subjects received. From Table I, the amount of noise apparent from the standard deviations of the measurements is much less for Subjects 1 and 2. Because the beat-by-beat method can detect quiescence in real-time, it serves as an important component of quiescence prediction from SCG in real-time.

The observed inter- and intra-subject variability of the quiescent period center with respect to the ECG suggests that ECG may be a suboptimal predictor of cardiac quiescence. A phase difference of 10% was shown to result in up to a 66% reduction in the total number of diagnostic studies for the subject population in [10]. The potential impact of the use of SCG for CT gating is an area of future research.

Composite velocity magnitude signals can be used to robustly detect the average quiescent periods for the range of heart rates observed for each patient. This method provides a convenient method for determining the optimal quiescent periods on average according to the SCG. Thus, patient-specific gating parameters can be obtained prior to a CTA examination and then utilized as optimal phases for gating by the CT machine. However, the performance of this type of patient-specific gating protocol is heavily dependent on intra-subject cardiac cycle variability because the composite signals are not sensitive to beat-by-beat variation in the motion of the chest wall.

Both of the presented methods serve an important role in the detection and prediction of cardiac quiescence. The beat-by-beat detection methods can be used for real-time prediction methods whereas the composite signal methods can be used for offline methods for predicting cardiac quiescence. Although offline methods are not as sensitive to beat-by-beat variability, they are a necessary first step toward SCG based gating because they can be implemented without any change in CT machine hardware. Future work will include assessing the accuracy of both the beat-by-beat and composite velocity methods by comparing the detected quiescent periods to those observed from CT data for the same patients. In addition, the potential increase in CT image quality resulting from more accurate gating will be investigated.

REFERENCES

[1] A. S. Go, D. Mozaffarian, V. L. Roger, E. J. Benjamin, J. D. Berry, W. B. Borden, D. M. Bravata, S. Dai, E. S. Ford, C. S. Fox, S. Franco, H. J. Fullerton, C. Gillespie, S. M. Hailpern, J. A. Heit, V. J. Howard, M. D. Huffman, B. M. Kissela, S. J. Kittner, D. T. Lackland, J. H. Lichtman, L. D. Lisabeth, D. Magid, G. M. Marcus, A. Marelli, D. B. Matchar, D. K. McGuire, E. R. Mohler, C. S. Moy, M. E. Mussolino, G. Nichol, N. P. Paynter, P. J. Schreiner, P. D. Sorlie, J. Stein, T. N. Turan, S. S. Virani, N. D. Wong, D. Woo, M. B. Turner, and American Heart Association Statistics Committee and Stroke Statistics Subcommittee, "Heart disease and stroke statistics–2013 update: a report from the American Heart Association." *Circulation*, vol. 127, no. 1, pp. e6–e245, Jan. 2013.

[2] J. M. Zanetti and D. M. Salerno, "Seismocardiography: a technique for recording precordial acceleration," in *Computer-Based Medical Systems, 1991, Proceedings of the Fourth Annual IEEE Symposium*, 1991, pp. 4–9.

[3] C. A. Wick, J. H. McClellan, A. E. Stillman, and S. Tridandapani, "A preliminary evaluation of the potential of seismocardiography as a gating tool for cardiac computed tomography," in *NASCI's 2011 Annual Meeting*, 2011.

[4] C. A. Wick, J. H. McClellan, O. brand, P. T. Bhatti, A. E. Stillman, and S. Tridandapani, "Variation between electrocardiographic and seismocardiographic signatures: implications for cardiac computed tomographic gating ," in *AMA-IEEE Medical Technology Conference 2011*, 2011.

[5] C. A. Wick, J.-J. Su, J. H. McClellan, O. brand, P. T. Bhatti, A. L. Buice, A. E. Stillman, X. Tang, and S. Tridandapani, "A system for seismocardiography-based identification of quiescent heart phases: implications for cardiac imaging," *IEEE Transactions on Information Technology in Biomedicine*, vol. 16, no. 5, pp. 869–877, 2012.

[6] R. E. Kalman, "A new approach to linear filtering and prediction problems," *Journal of basic Engineering*, vol. 82, no. 1, pp. 35–45, 1960.
[7] G. Bishop and G. Welch, "An introduction to the Kalman filter," *Proc of SIGGRAPH, Course*, vol. 8, pp. 27 599–23 175, 2001.
[8] M. Di Rienzo, E. Vaini, P. Castiglioni, G. Merati, P. Meriggi, G. Parati, A. Faini, and F. Rizzo, "Wearable seismocardiography: towards a beat-by-beat assessment of cardiac mechanics in ambulant subjects." *Auton Neurosci*, vol. 178, no. 1-2, pp. 50–59, Nov. 2013.
[9] K. R. Johnson, S. J. Patel, A. Whigham, A. Hakim, R. I. Pettigrew, and J. N. Oshinski, "Three-dimensional, time-resolved motion of the coronary arteries," *J Cardiovasc Magn Reson*, vol. 6, no. 3, pp. 663–673, 2004.
[10] M. B. Srichai, E. M. Hecht, D. Kim, J. Babb, J. Bod, and J. E. Jacobs, "Dual-source computed tomography angiography image quality in patients with fast heart rates," *J Cardiovasc Comput Tomogr*, vol. 3, no. 5, pp. 300–309, Sep. 2009.